



This is a repository copy of *The European Solar Telescope (EST)*.

White Rose Research Online URL for this paper:
<http://eprints.whiterose.ac.uk/154529/>

Version: Published Version

Proceedings Paper:

Matthews, S.A., Collados, M., Mathioudakis, M. et al. (1 more author) (2016) The European Solar Telescope (EST). In: Evans, C.J., Simard, L. and Takami, H., (eds.) Ground-based and Airborne Instrumentation for Astronomy VI. SPIE Astronomical Telescopes + Instrumentation, 26-30 Jun 2016, Edinburgh, UK. SPIE . ISBN 9781510601956

<https://doi.org/10.1117/12.2234145>

Sarah A. Matthews, Manuel Collados , Mihalis Mathioudakis, and Robertus Erdelyi "The European Solar Telescope (EST)", Proc. SPIE 9908, Ground-based and Airborne Instrumentation for Astronomy VI, 990809 (3 August 2016);
<https://doi.org/10.1117/12.2234145>

Reuse

Items deposited in White Rose Research Online are protected by copyright, with all rights reserved unless indicated otherwise. They may be downloaded and/or printed for private study, or other acts as permitted by national copyright laws. The publisher or other rights holders may allow further reproduction and re-use of the full text version. This is indicated by the licence information on the White Rose Research Online record for the item.

Takedown

If you consider content in White Rose Research Online to be in breach of UK law, please notify us by emailing eprints@whiterose.ac.uk including the URL of the record and the reason for the withdrawal request.



eprints@whiterose.ac.uk
<https://eprints.whiterose.ac.uk/>

The European Solar Telescope (EST)

Sarah A. Matthews^{*a}, Manuel Collados^b, Mihalis Mathioudakis^c, Robertus Erdelyi^{d,e}, and the EST Team

UCL-Mullard Space Science Laboratory, Holmbury St. Mary, Dorking Surrey RH5 6NT, UK^a;

^bInstituto de Astrofísica de Canarias, c/Vía Lactea s/n, La Laguna 38205, Tenerife, Spain;

^cAstrophysics Research Centre, School of Mathematics and Physics, Queen's University Belfast, BT7 1NN, Northern Ireland, UK; ^dSolar Physics and Space Plasma Research Centre (SP2RC), School of Mathematics and Statistics, University of Sheffield, Hicks Building, Hounsfield Road, Sheffield, S3 7RH, UK; ^eDebrecen Heliophysical Observatory (DHO), Research Centre for Astronomy and Earth Sciences, Hungarian Academy of Science, 4010 Debrecen, P.O. Box 30, Hungary

ABSTRACT

The European Solar Telescope (EST) is being designed to optimize studies of the magnetic coupling between the lower layers of the solar atmosphere (the photosphere and chromosphere) in order to investigate the origins and evolution of the solar magnetic field and its role in driving solar activity. In order to achieve this, the thermal, dynamic and magnetic properties of the solar plasma must be probed over many scale heights and at intrinsic scales, requiring the use of multi-wavelength spectroscopy and spectropolarimetry at high spatial, spectral and temporal resolution. In this paper we describe some of the over-arching science questions that EST will address and briefly outline the main features of the proposed telescope design and the associated instrumentation package.

Keywords: solar telescopes; high resolution imaging; high resolution spectroscopy; solar spectropolarimetry

1. INTRODUCTION

The Sun is our closest star, and with space now firmly established as a critical part of our society's environment, its unique proximity has inescapable consequences for us. While its radiation provides the energy source of our whole ecosystem, our understanding of how the variations in that radiation control, e.g. our climate, still contains huge gaps. As well as the long-term variations in the solar output, the Sun exhibits a cycle of activity the constituents of which are explosive events which release huge amounts of magnetic energy that are subsequently converted to many other forms. This explosive energy release occurs on a myriad of scales, from nanoflares to huge eruptive flares, the latter accompanied by the bulk eruption of plasma and magnetic field known as coronal mass ejections (CMEs) whose impacts can be seen globally across the Sun and throughout the heliosphere. The most extreme of these events constitute the largest examples of explosive energy release within our solar system, during which upwards of 10^{26} J of energy is released.

The ramifications of these explosive events within the heliosphere and the near-Earth environment are considerable. The increased electromagnetic radiation produces significant changes in the Earth's upper atmosphere that impact communications and satellite orbits, with 'immediate' consequences for GPS L-band signals. The fluxes of accelerated particles that are produced during solar energetic particle events (SEPs) lead to significantly increased ionisation in the polar atmosphere, affecting radio transmissions and the chemistry of the upper atmosphere. Particularly for large events, ozone levels can be subsequently affected for months and even years [1]. SEPs also present a high risk to both manned and un-manned space platforms, while the interactions between the magnetic field of the CME and our own magnetosphere can lead to well documented impacts on Earth.

Our ability to probe many layers of the solar atmosphere simultaneously offers unique opportunities to understand the processes that drive these explosive events, and study the relationship between fundamental physical processes such as

magnetic reconnection, wave generation and particle acceleration. As well as a desire to understand how these processes operate and couple in order to develop reliable tools for the prediction of solar flares & CMEs, these are the same processes also operating in other astrophysical environments. On the Sun we have the possibility to observe and map the evolving magnetic field configuration where the energy release, particle acceleration and subsequent energy transport, takes place, and only by fully understanding this parameter space can we begin to appreciate how these processes are operating in other more extreme astrophysical environments, as well as critically assess how they might effect the formation of life on planets outside of our own solar system.

To understand the Sun's activity we need to observe and model the physical processes in the solar atmosphere at their intrinsic spatial and temporal scales. The EST is a pan-European project whose goal is the design and construction of a revolutionary 4-m diameter ground-based solar telescope and its post-focus instrumentation suite in order to answer these science questions. From its first-light in 2026 EST will become the primary ground-based European solar facility. Its novel adaptive optics will enable diffraction-limited observations with an unprecedented spatial resolution of 30 km, less than the photon scattering mean free path in the photosphere, a fundamental physical scale in the visible. Perhaps most importantly, EST will not only make a step change in achievable spatial resolution, but crucially its polarimetric capabilities will allow the simultaneous observation of the temporal and spatial evolution of the three dimensional magnetic field in the solar photosphere and chromosphere, allowing us to understand the emergence and evolution of the solar magnetic field, and critically, to understand the coupling between the photosphere and chromosphere.

2. SCIENCE GOALS

EST will answer fundamental questions relating to the origins of solar magnetism. In particular it will address:

The role of small-scale field concentrations in the evolution of the solar magnetic field throughout the solar cycle: Outside sunspots, the solar magnetic field is organized in small-scale magnetic flux concentrations with spatial scales down to the diffraction limit of current solar telescope (<100 km). These concentrations are believed to play an important role in controlling solar irradiance, as well as in the dynamics and, ultimately, the heating of the chromosphere and corona through a variety of localised processes, including the channelling of waves and shocks. The field in these magnetic flux concentrations can reach values of up to 1.5 kG, requiring a field amplification process. One possibility is a process known as convective collapse, which leads to a strong evacuation of a magnetic flux tube and a concentration of the magnetic field, coupled to rapid downflows both in the tube's interior and its surroundings. The associated spatial and temporal scales are on the order of 100 km and 30 s, according to state-of-the-art numerical simulations. Observational evidence to support this process has proven challenging, partly because current polarimetric measurements cannot meet the very small scales and rapid cadences required. EST will resolve some of the smallest magnetic field concentrations, which are ubiquitous across the solar disk, down to the 25 km diffraction limit, and track their emergence, structure and dynamics and, perhaps most importantly, measure their three-dimensional vector magnetic field. Its field-of-view will accommodate features of the global field — the sunspots and active regions that are generated by a large-scale sub-surface dynamo, and emerge by buoyancy to the photosphere.

Establishing how energy is transported from the photosphere to the chromosphere. Despite many years of research, the reasons why the average electron temperature in the solar atmosphere begins to increase again about ~500 km above the solar surface, giving rise to a warm chromosphere, a hot and dynamic transition region, and even hotter corona above, are still unknown. The strong radiative losses of the chromosphere and transition region make its energy requirements much more demanding than for the corona, and the current consensus is that the additional energy comes from the turbulent convective plasma motions that penetrate through the photosphere. One of the most promising mechanisms by which this energy could be transported to the chromosphere is by magnetohydrodynamic waves, with dissipation in the form of chromospheric shocks, or other complex processes in magnetically dominated regions (e.g. phase mixing, resonant absorption). However, the chromosphere represents a region of vast changes in plasma properties - the gas pressure falls exponentially with a scale height of ~200 km, while the magnetic field strength falls off much less rapidly, as it expands and fills all space, i.e. the transition from high to low plasma- β occurs in the mid chromosphere. Thus, while the lower chromosphere shares many characteristics with the photosphere, the upper chromospheric structure is dominated by the magnetic field topology and strength, leading to intricate patterns of wave interactions that are highly variable in space and time. The detection of periodic signatures in line profiles (i.e. Doppler broadening and Doppler shifts), combined with measurements of the direction and strength of the magnetic field, is critical in order to identify

and characterize wave modes and their propagation in the lower solar atmosphere, requiring simultaneous observation of several photospheric and chromospheric spectral lines. The topology, strength, and flux evolution of the magnetic fields must also be measured with high spatial, temporal and spectropolarimetric precision. EST's light-gathering capacity and polarimetric precision is vital for detecting the three dimensional structure of the weak chromospheric magnetic field and disentangling its morphology and dynamics down to the smallest scales observable.

Determining what processes are involved in the large-scale release of energy in flares and CMEs. The study of solar flares and accompanying Coronal Mass Ejections (CMEs) is a topic of fundamental importance in solar and space physics research, not just for our understanding of solar activity and its impacts on the near Earth space environment (space weather), but also from the perspective of energy release in astrophysical plasmas in general. In particular, the physics of energy storage, flare triggering and flare energy release remains an enigma that extends beyond the predictions of our current flare models. Magnetic free energy is known to arrive into the corona through the photosphere, a process which may be tracked by emergence and flows in photospheric magnetic structures, revealing where the emerging flux is introducing magnetic twist into the overlying field or cancelling and changing the topology of a pre-existing flux system in the build-up of an instability. While solar flares and eruptions have a dramatic coronal appearance, the majority of the energy that they radiate (which forms the basis of the majority of the diagnostics available to us) is in fact radiated from the transition region, chromosphere and photosphere. Flare signatures in the lower atmosphere map directly to the energy release sites in the corona, making this regime one of critical importance to understanding both the onset and evolution of both flares and CMEs. EST will address the arrival and deposition of flare energy in the lower solar atmosphere by revealing the basic spatial scales of flare energy input and its vertical location in the atmosphere. EST will also provide accurate magnetic field measurements from the photosphere into the chromosphere, allowing the determination of pre- and post- flare & CME configurations. Its photospheric and chromospheric imaging and spectroscopic capabilities will provide critical information on the topological changes in the magnetic field as a result of magnetic reconnection. EST will also enable the detailed study of the magnetic and thermodynamic properties of the filaments that form the core of many CMEs, including their formation.

3. BASELINE CONFIGURATION

The planned design for EST is a 4-metre class telescope with on-axis Gregory configuration. Active and adaptive optics (AO) will be integrated into the optical path between the primary mirror and the focal plane in order to simultaneously provide all instruments with a corrected image at the Coudé focus. Since the original design study it has been envisaged that EST will be the first solar telescope to fully integrate multi-conjugate adaptive optics (MCAO) into the optical path from construction. The adaptive optics system will include a fast tip-tilt mirror, a pupil deformable mirror and four deformable mirrors conjugated at different atmospheric heights.

The optical design is an aplanatic Gregory telescope with three magnification stages, giving an f/50 telecentric science focus [2]. In order to optimize the telescope to achieve polarization compensation, integrated optical field-of-view rotation, telecentric design, collimated beam at the AO system and four MCAO DM mirrors [3], the design includes fourteen reflections arranged so that incidence-reflection planes are perpendicular. The alt-azimuth configuration allows for a compact design, with excellent primary mirror (M1) air flushing, making it possible to achieve a polarimetrically compensated design, critical for achieving the science goals. In order to facilitate the M1 air flushing, the elevation axis is cited 1.5 m below the M1 vertex, and this also provides space for vertical placement of the transfer optics train to the Coudé focus. The unbalanced weight around the elevation axis that this produces is compensated for by the structure below M1. Asymmetric folding of the optical path produces a telescope Mueller matrix that is almost independent of elevation and azimuth angles for all wavelengths, but requires that the azimuth and elevation axes are decentred with respect to the telescope optical axis.

A large Coudé laboratory allows for the different instruments to be situated on different floors, fed by a configurable light distribution system composed of dichroics and beam-splitters at the Coudé focus. This allows for maximum flexibility in the number of instruments and wavelength channels. Image rotation is also compensated at the Coudé focus through the placement of an optical de-rotator integrated into the telescope optical path. In order to achieve this, the seven mirrors of the transfer optics are arranged in such a way that input and output optical axes are coincident with the telescope optical axis, allowing them to be rotated around it to act as a de-rotator. This arrangement has the added bonus

that it removes the requirement for a rotating instrument platform. An auxiliary Nasmyth platform will also be available for NIR or UV instruments to be fed directly from the telescope.

The baseline telescope enclosure is completely foldable [2], in order to maximize natural wind flushing of the telescope, and improve the local seeing conditions. An additional and important advantage of the completely foldable enclosure is that it permits the use of a reflecting heat rejecter at the Gregory focus, thereby removing the requirement to absorb the heat inside the dome. The open-air configuration has implications for image quality as the result of wind-shake on the telescope structure and wind buffeting deformation of the primary mirror. This issue has been compensated for by inclusion of a wind shield, and by maximizing the stiffness of the telescope structure and primary mirror support, improving the bandwidth of the telescope drives, and providing fast tip-tilt and focus correction capabilities to the secondary mirror. Residual wind generated errors can be corrected by the deformable mirrors of the AO system.

In order to improve seeing, the telescope will be placed on the top of a conically shaped tower that also supports the telescope enclosure. The enclosure is supported with a transparent framework, to reduce air obstruction and turbulence, and the optical layout is arranged on a tower situated ~33–38 m between the base of the Coudé laboratory and the telescope platform, sufficient to reduce the ground layer effect on the local seeing conditions. The Coudé instrument laboratory will be situated at the base of the tower, while the transfer optics, including the MCAO system, will be distributed inside a chamber between the telescope and the instrument laboratory. The baseline construction material for the telescope tower is concrete, which will provide the necessary stiffness to the telescope azimuth base, and minimize both lateral displacement and the tilt between the telescope and the Coudé focus.

An auxiliary full disk telescope [4] will be used to give the observer a global context of the solar activity and allow for precise coordinate measurements. The operation of the telescope will be carried out by an integrated control system, employing distributed, object-oriented architecture and common software throughout the entire system. The volumes of data that EST will produce require a highly efficient control system for management of the data and metadata, and their transmission from each sub-system to a real-time repository, as well as to users and to temporary and permanent archives [5]. Figure 1 shows the proposed realization of the telescope and the facilities that host it.

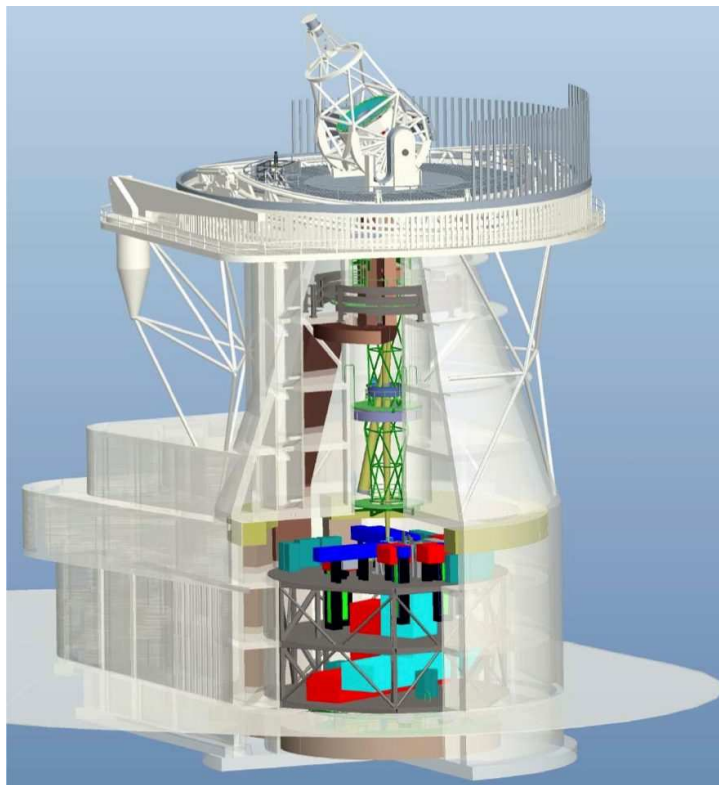


Figure 1: Schematic of the telescope structure, instrument platform, pier and building from [3].

4. OPTICAL DESIGN

As noted above, the main telescope has an on-axis Gregory-type configuration (see [2]) achieving a diffraction-limited Coudé Focus in the range 0.39 μm to 2.3 μm . The optical design of EST is composed of three main subsystems (see Fig. 2):

1. Main telescope (M1 and M2), defined by an on-axis Gregory-type configuration.
2. Main axes subsystem (M3 to M8), which includes mirrors that define the elevation and azimuth axes. This subsystem houses an on-axis magnification stage to produce the pupil used by the AO system.
3. Transfer optics subsystem (M9 to M14). These mirrors transfer the light from the main axes subsystem to the science Coudé Focus. This assembly integrates the MCAO mirrors in its light path and also works as the field-of-view de-rotator of the telescope.

The main telescope includes an $f/1.5$ primary mirror. The secondary mirror defines the aperture stop of the whole system and produces an $f/11.8$ beam at the secondary focus (F2). A heat rejecter that also works as a field-stop is located at the primary focus (F1) to limit the field of view to the required unvignetted 2×2 arcmin². The entrance pupil of the system is defined by the conjugation of the aperture stop (M2) through M1, and is 4100 mm in diameter. Active optics correction is achieved by mounting M2 on a hexapod [6] with 5 degrees of freedom (piston, δx , δy and slow tip-tilt). Additionally, M2 can be used as a fast AO tip-tilt mirror, with a limited bandwidth. If a larger bandwidth is required, a second smaller and faster tip-tilt mirror, M6 (which is located in the main axes subsystem), will be used. Including fast tip-tilt and piston capabilities at M2 will provide adaptive correction for the Nasmyth station.

To further facilitate polarization compensation within the telescope, M3 and M4 will have identical reflection coatings, and will be tilted 45 degrees in perpendicular planes to auto-balance their instrumental polarization. The ground-layer turbulence correction is also accomplished within the main axes subsystem.

4.1 Adaptive Optics

To achieve the required high spatial resolution, it is necessary for EST to incorporate a powerful adaptive optics system [7,8]. The adaptive optics system will include a ground layer adaptive optics system (GLAO), composed of a deformable mirror located at a pupil position, and a fast tip-tilt mirror, as well as additional deformable mirrors that are required to increase the size of the corrected field of view. These DMs will be located at positions that correspond to certain heights in the atmosphere, thus achieving a multi-conjugate system. Without a multi-conjugate adaptive optics system it would not be possible to achieve the required corrected FoV. The AO system will be integrated in the main telescope optical path in order to minimize the number of optical surfaces.

4.2 Ground Layer Adaptive Optics

The GLAO is composed of the pupil DM and the tip-tilt mirror, with the pupil DM (M7) located at a pupil position. The optimum sub-aperture size has been determined to be 8 cm, which is equivalent to 50 sub-apertures across the pupil mirror, and hence 51 actuators across the DM diameter. Approximately, 50% of the stroke of the actuators will be dedicated to compensating for atmospheric effects and 50% to telescope effects.

The tip-tilt mirror can be implemented at either M2 or M6, with M2 defining the telescope pupil and including fast tip-tilt and focus capabilities in order to provide some wave-front correction to the Nasmyth focus. The M2 fast tip-tilt and focus correction capabilities are intended to compensate for a large fraction of the wave-front distortions produced by the effects of wind buffeting on M1, since they are also capable of correcting for piston and focus errors, in addition to the tip-tilt components. These capabilities are also useful for the Coudé path, since they reduce the load on the rest of the AO system. However, given the relatively large diameter of M2 (800 mm), its correction bandwidth will be limited. For this reason, the possibility of implementing a second smaller and faster tip-tilt mirror at M6 is being investigated.

4.3 MCAO

The driver for the MCAO optical design (in particular the number and size of the conjugate high altitude DMs) is the turbulence (Cn2) stratification with height above the telescope site. The large zenith angles that are typical of solar

observations during the morning lead to a variation in the effective turbulence over a wide range of heights. EST's solution to this is a configuration based on four conjugated DMs (M9-M12) at fixed positions, that reduce the height mismatch between the DMs and the turbulence layers caused by the varying zenith angle. The optical design allows some flexibility to adapt the position of the conjugated DMs without dramatic changes in the optical layout.

Given the size of the telescope and primary mirror, the telescope must include active optics in order to keep the alignment and optical figure of the mirror. These will compensate for initial alignment tolerances, changes in the gravity vector with elevation angle, temperature variations and wind buffeting. In order to guarantee the optical quality of the telescope, continuous operation of the active optics system will be required throughout the telescope operation.

5. INSTRUMENTS

The EST instrumentation suite is preliminary at this stage, but will comprise a range of instruments devoted to imaging, spectroscopy and spectropolarimetry, with the instruments distributed across two floors in the Coudé laboratory: the upper one dedicated to imagers, and the lower one to grating spectrographs. The instrument layout within the Coudé laboratory takes into account the current design of each instrument type, as well as the possibility of adding two additional guest instruments (one in the visible beam and one in the NIR beam).

The design of the Coudé laboratory has the instruments static on a concrete slab (field rotation being provided by transfer optics as described above). The light coming from the telescope is then split between the following instruments channels:

- Three visible broad-band imaging channels [9].
- Five narrow-band imager channels: three operating in visible wavelengths and two in the near-infrared (NIR).
- Four grating spectrographs: two for the visible spectral range and two for the NIR. These spectrographs are envisaged to have flexible modes of operation, allowing for the following possible configurations [10]:
 - Long-slit standard spectrograph.
 - Multi-slit multi-Wavelength spectrograph equipped with an integral field unit [11].
 - Tunable universal narrow-band imaging spectrograph.
 - Multi-channel subtractive double-pass spectrograph of new generation.

The light distribution among the instruments (see Fig. 2) is based on a division of the main beam coming from the transfer optics by a primary dichroic D1 in two spectral stations: one for visible wavelengths and another for near-infrared. This division makes it possible to optimize the light flux transmission (after the beam separation, coating optics can be optimized for the selected spectral range at each station).

After the intensity beam-splitter BS5, the transmitted beam goes to the scanning unit of the two NIR spectrographs (a single unit for both). This unit is based on two pairs of 45-incidence mirrors, for which the lines that connect the centre of the mirrors of each pair are perpendicular to each other. This means that the FoV of the telescope can be scanned in both directions to select the spectrograph FoV without impacting the imaging instruments. For the visible branch, one similar quad-mirror is located in the beam reflected by BS1 to scan the entrance FoV of the visible spectrographs. In addition, these quad-mirror scanning systems can also focus the image at the entrance focal plane of the spectrographs. Below we briefly describe only the currently envisaged designs for the broadband imager and the multi-slit multi-Wavelength spectrograph equipped with an integral field unit [11].

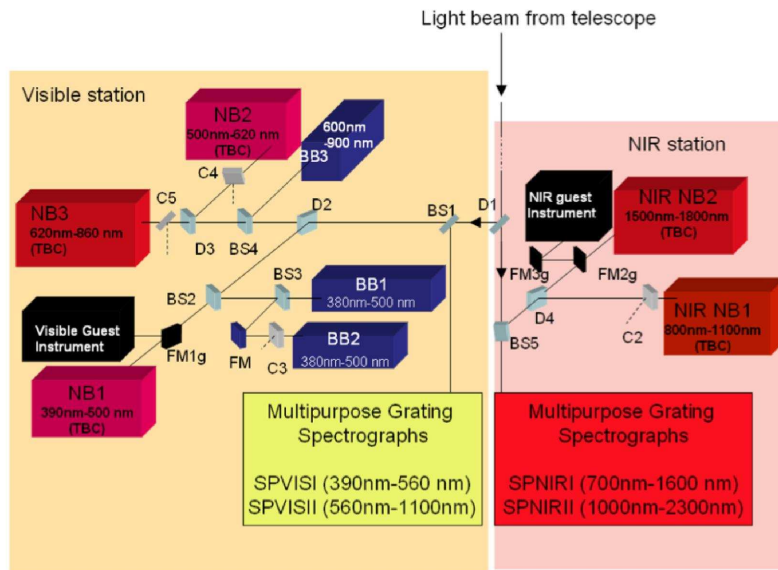


Figure 2: Light distribution for the instruments of EST. Labels Dn correspond to dichroic mirrors splitting light in wavelength; labels BSn stand for intensity beam-splitters, and labels FM refer to folding mirrors. BBn indicate the broad-band imagers, NBn the narrow-band instruments and SPn the spectrographs (from [3]).

5.1 Broadband Imager (BBI)

The BBI will be a pivotal baseline instrument for EST, exploiting the high spatial and temporal resolution afforded by a 4 metre class telescope. The requirements for the instrument are given in Table 1, but in addition the final instrument design should include the capability for each wavelength channel to work as a ‘stand-alone’ instrument, and allow for the use of post-fact reconstruction methods (e.g. SPECKLE [12]; MOMBFD [13]) in order to achieve diffraction limited imaging, i.e. three focal planes and associated detectors are required: two chromospheric channels for phase diversity, and a third continuum channel to correct the chromospheric data.

In order to achieve the multi-channel requirements of the BBI, the instrument will have two arms: red (600-900 nm) and blue (390-500 nm), with the latter split into two channels. Beam-splitters and dichroics will allow simultaneous use of all channels. Further details can be found in [10].

Table 1: Requirements for the EST broad-band imager (adapted from [10]).

No. spectral channels	3 channels working simultaneously; goal - 5
Max. FoV	2x2 arc minutes
Angular resolution	0.04" @ 500 nm (goal: 0.03") over a 60"x60" FoV
Mosaic mode	3'x3' mosaic mode at optimum resolution (60"x60" sub fields)
Wavelength coverage	390 – 900 nm
Wavelength switching	< 2 seconds
Max. bandpass shift	5×10^{-3} nm (goal: 3×10^{-3}) @ 500 nm, 30" from field centre
Transmission	Total throughput > 30%

5.2 Grating Spectrograph

Spectroscopy and spectropolarimetry are primary tools for diagnosing the state of the solar plasma and the electric and magnetic fields that permeate it, and thus spectrographs are key instruments for EST. A very desirable evolution of the current state of the art in solar spectrographs is to combine spectroscopic and spectro-polarimetric functions within a single instrument, which also addresses the limitations in simultaneity imposed by scanning slit spectrographs. This is precisely the concept proposed by [11] through the application of integral field spectroscopy. The instrument requirements are listed in Table 2, and reflect the scientific requirements to be able to resolve structures of ~ 70 km in the photosphere and the chromosphere with a spectral resolution of 300000 across a spectral range covering 390 – 2300 nm. The proposed spectrograph configuration allows the simultaneous observation of eight wavelengths (five visible and three infrared) meaning that energy transport and coupling between different layers of the solar atmosphere can be, for the first time, accurately tracked. The spectrograph incorporates a new concept integral field unit based on the image slicer concept developed by [14]. While now being more routinely considered for night-time astronomy applications, image slicers are a new technology for solar telescopes. The DL-NIRSP (Diffraction Limited Near Infrared Spectrograph) currently being developed for the Daniel K. Inoué Solar Telescope (DKIST [11]) includes an image slicer in its design, but covers only the range 500 -1800 nm in three spectral windows. The proposed design for EST would represent a step change in spectroscopic and spectropolarimetric capabilities for solar physics. Further details can be found in [11].

Table 2: Integral field spectrograph requirements, from [11].

Spectral resolving power	300,000
Spatial resolution	0.1"
Spectral range	390 – 2300 nm
Number of simultaneous wavelengths	8, 5 visible, 3 NIR

6. SUMMARY

In summary, once constructed, EST will be the state-of-the-art ground-based solar telescope in Europe, and will possess the most powerful spectropolarimetric capabilities of any solar facility, in space or on the ground. It will be highly complementary to the US DKIST facility, but will benefit from the integration of MCAO from construction, and access to the most advanced instrumentation suites. EST will make major contributions to resolving the outstanding open questions in solar physics.

7. REFERENCES

- [1] Jackman, Charles H.; Fleming, Eric L.; Vitt, Francis M., "Influence of extremely large solar proton events in a changing stratosphere", JGR, 105, D9, 11659-11670, (2000).
- [2] Sánchez-Capuchino, J., Collados, M., Soltau, D. et al., "Current concept for the 4m European Solar Telescope (EST) optical design", Proc. SPIE, 7733, 773336, (2010).
- [3] Bettonvil, F. C. M., Collados, M., Feller, A., et al., "The Polarization Optics for the European Solar Telescope", ASPC Proceedings, Solar Polarization 6, 437, 329, (2011).
- [4] Sobotka, M., Klvanã, M., Melich, Z., et al., "Auxiliary full-disc telescope for the European Solar Telescope", Proc. SPIE, 7735, 77351Z, (2010).
- [5] Ermolli, I., Bettonvil, F., Cauzzi, G., et al., "Data handling and control for the European Solar Telescope", Proc. SPIE, 7740, 77400G, (2010).

- [6] Cavaller, L., Siegel, B., Prieto, G., et al., "Secondary mirror system for the European Solar Telescope (EST)", Proc. SPIE, 7739, 77392O, (2010).
- [7] Berkefeld, T., Soltau, D., Del Moro, D., & Löfdahl, M., "Wavefront sensing and wavefront reconstruction for the 4m European Solar Telescope EST", Proc. SPIE, 7736, 77362J, (2010).
- [8] Soltau, D., Berkefeld, T., Sánchez Capuchino, J., et al., "Adaptive optics and MCAO for the 4-m European Solar Telescope EST", Proc. SPIE, 7736, 77360U, (2010).
- [9] Munari, M., Scuderi, S., & Cecconi, M., "Broad band imager for the European Solar Telescope", Proc. SPIE, 7735, 773560, (2010).
- [10] Calcines, A., Collados, M., Feller, A., et al., "Spectrograph capabilities of the European Solar Telescope", Proc. SPIE, 7735, 773520, (2010).
- [11] Calcines, A., Collados, M., & López, R. L., "Conceptual design of a high-resolution, integral field spectrograph for the European Solar Telescope", Highlights of Spanish Astrophysics VI, 660, (2011)
- [12] Wöger, F.; von der Lühe, O.; Reardon, K., "Speckle interferometry with adaptive optics corrected solar data", A&A, 488, 375-381, (2008).
- [13] Van Noort, Rouppe Van Der Voort, L., Lfdahl, M.G., "Solar Image Restoration by use of multi-frame blind deconvolution with multiple object", Solar Physics 228, 191- 215, (2005)
- [14] Calcines, A.; López, R. L.; Collados, M., "MuSICa: the Multi-Slit Image Slicer for the EST Spectrograph", Journal of Astronomical Instrumentation, 2, 1350009, (2013).

8. ACKNOWLEDGMENTS

This work has been carried out as a part of several EC funded projects supporting the development of EST, including: Collaborative Project EST: The large-aperture European Solar Telescope, Design Study, funded by the European Commission's 7th Framework Programme under grant agreement no. 212482; SOLARNET, also funded by the European Commission's 7th Framework Programme under grant agreement 312495, and GREY: Getting Ready for EST, funded by the European Commission's Horizon 2020 programme under grant agreement 653982. EST is promoted by the European Association for Solar Telescopes (EAST), formed by 15 research institutions from Austria, Croatia, Czech Republic, France, Germany, United Kingdom, Hungary, Italy, The Netherlands, Norway, Poland, Slovakia, Spain, Sweden and Switzerland.